JOURNAL OF SOLID STATE CHEMISTRY 49, 289–299 (1983)

Ion-Exchange Reactions of Mixed Oxides

W. A. ENGLAND,[1] J. B. GOODENOUGH, AND P. J. WISEMAN

Inorganic Chemistry Laboratory, South Parks Road, Oxford OX1 3QR, United Kingdom

Received March 9, 1983

Ion-exchange reactions are described for a range of mixed oxides, including the layered α-$NaCrO_2$ structure, the $Rb_2Ti_6O_{13}$ tunnel structure, and a spinel phase. The rates of the ion-exchange reactions are consistent with the kinetic theory derived for classical ion-exchange materials and are compatible with the low ionic conductivities observed. Ion-exchange reactions, particularly with molten salts, are shown to be a general feature of many inorganic solids; they offer a preparative route to new, commonly metastable, materials.

1. Introduction

Ion-exchange reactions, carried out in an aqueous exchange medium, have been extensively studied for "classical" ion exchangers such as zeolites, micas, acid phosphates, hydrous oxides and sulfonic acid resins. The ease of ion exchange in these materials may be understood in terms of the presence of interconnected cages, channels, or layers of sufficient dimensions to allow ion transport. Easily expandable materials, such as the hydrous oxides and poorly crosslinked sulfonic acid resins, can accommodate hydrated cations and are fast, but relatively unselective, exchangers. Ionic mobility within the solid may be similar in mechanism and magnitude to that of a free aqueous solution. Crosslinked zeolites may necessitate "anhydrous" ion exchange and are, as a consequence, usually slower, but more selective. Cation transport in these materials should have a mechanism more typical of solids where an activated cation hopping to vacant sites occurs through well defined anion-bounded "bottlenecks."

So-called "fast ion conductors," such as the β-aluminas (*1*), represent a new series of ion exchangers with accentuated zeolitic properties. The partially occupied, interconnected channels permit rapid, anhydrous ion exchange; and exchange may be carried out in both aqueous and molten salt conditions. However, most studies have concentrated on the ionic transport properties of these materials. The purpose of this paper is to examine further the relationship between these two large disciplines. Two questions are of particular interest. What range of diffusion coefficients and ionic conductivities are shown by compounds exhibiting ion exchange? Which structures are likely to show ion-exchange reactions? The exchange process has two separate aspects. The thermodynamics of exchange will favor exchange with ions of comparable size, unless the material is readily ex-

[1] Present address: Materials Physics Division, A.E.R.E. Harwell, Didcot, Oxon, OX11 ORA, United Kingdom.

0022-4596/83 $3.00

pandable. Identical charges, however, may not be necessary. Substitution with an ion of higher charge can be achieved by creation of ion vacancies. Conversely, if ion vacancies are already present, a degree of exchange with an ion of smaller charge is possible. The equilibrium extent of exchange is then determined by the appropriate equilibrium selectivity coefficient and the concentration ratio of in-going and out-going ions. Certain ion-exchange reactions should be thermodynamically feasible for many solid state structures.

The kinetic aspect of an ion-exchange reaction is a much more stringent criterion. The ion-exchange kinetic theory of Boyd *et al.* (*2*), first presented in 1947, and extended by Reichenberg in 1953 (*3*), provides much assistance. The rate determining step was shown to be diffusion within the solid provided an excess of well-stirred, concentrated exchange liquid was used. For spherical particles of radius r and a fixed fraction of exchange $f = F(t)/F(\infty)$, the theory predicts a relationship between the exchange time t and the chemical interdiffusion coefficient D_i for the in-coming and out-going ions:

$$f = 1 - (6/\pi^2) \sum_{n=1}^{\infty} [\exp(-n^2Bt)]/n^2$$

where $B = \pi^2 D_i/r^2$.

It should be emphasized that this expression represents the rate of attainment of a specific fraction of the equilibrium extent of exchange represented by $F(\infty)$. The latter will be a large or small proportion of the total possible exchange capacity of the material and will be dependent on the thermodynamic factors described earlier. The above relationship implies that there is a characteristic time $\tau = r^2/D_i$ taken to achieve a given fraction of exchange. A large interdiffusion coefficient and small solid particles favor a rapid exchange process. The effective value of r may be much less than the geometrical value in the case of cracked or irregular particles. In practice, ion exchange often causes fragmentation of solids due to lattice parameter changes; such fragmentation accelerates ion exchange. Values of t are calculated for various values of D_i in Table I for the case of spherical particles of radius 100 μm and $f = 0.95$. Some typical diffusion coefficients and activation energies are also shown. It should be noted, of course, that D_i is strictly a mixed chemical diffusion coefficient with $D_i = D_{i0}\exp(-\Delta H_m/kT)$, where ΔH_m is the enthalpy change for a mixed ion jump.

The implications from Table I are clear. First, ion exchange is a necessary, but not sufficient, condition for fast ion conduction. Only if ion exchange is extremely rapid, as may occur in practical exchangers, are diffusion coefficients typical of fast ion conductors necessitated ($\approx 10^{-7}$ cm^2 sec^{-1}). This relationship has been exploited in finding new fast proton conductors (*4*). Secondly, with exchange times of a few days, ion exchange of small particles may be observed for diffusion coefficients at the exchange temperature as low as $\approx 10^{-12}$ cm^2 sec^{-1}. The values quoted for the Na^+ ion diffusion coefficient in NaCl at various temperatures (*5*) indicate that ion-exchange reactions may be quite a widespread phenomena of inorganic solids at temperatures well below sintering temperatures; they also emphasize that substantial concentrations of mobile-ion vacancies (introduced by nonstoichiometry or doping) may not be necessary.

This paper reports some preliminary investigations to test these predictions. We have chosen nominally stoichiometric, mixed metal oxides of different structural characteristics as the more stringent test. Since one objective of this study is the preparation of phases not accessible by high temperature reactions, it is important to recognize that ion-exchange reactions

TABLE I

TIME t TO ACHIEVE $F(t)/F(\infty) = 0.95$ FOR SPHERICAL PARTICLES OF RADIUS $r = 100\ \mu m$

D (cm^2 sec^{-1})	10^{-5}	10^{-7}	10^{-9}	10^{-10}	10^{-11}	10^{-12}
t	2.5 sec	4.2 min	6.9 hr	69 hr	29 days	290 days

	D (cm^2 sec^{-1})	ΔH_m (kJ mole^{-1})
Na^+ in molten NaCl (1300 K)	2.1×10^{-3}	30
Li^+ in 1 M LiCl(aq)(300 K)	1.3×10^{-5}	—
Na^+/Li^+ in Amberlite IR1 (300 K)	3.0×10^{-6}	—
Na^+ in Na β-alumina (300 K)	4.0×10^{-7}	16
Na^+ in Na β-alumina (600 K)	1.8×10^{-6}	16
NH_4^+/NEt_4^+ in phenolsulfonic acid (300 K)	5.0×10^{-9}	21
Na^+ in NaCl (intrinsic region, 900 K)	1.0×10^{-10}	173
Na^+ in NaCl (extrinsic region, 650 K)	1.0×10^{-12}	74
Na^+/Tl^+ in analcite (373 K)	4.5×10^{-13}	62

that result in metastable phases must be carried out at temperatures that are too low for the ions of the framework structure to reconstruct themselves into their stable configuration. In other words, the exchange must be accomplished at temperatures well below sintering temperatures.

2. Structures Investigated

A. Layered $A^IB^{III}O_2$ Structures

The layered $A^IB^{III}O_2$ structures contain infinite sheets of edge shared BO_6 octahedra (Fig. 1) interleaved with layers containing exclusively A atoms. Different layer stacking sequences produce different coordinations of the A atoms and give rise to various ABO_2 structures. In the α-$NaCrO_2$ structure (*6*), the A atoms are octahedrally coordinated with an (*ABC* . . .) oxygen packing sequence (Fig. 2). This may be regarded as an ordered NaCl structure with A and B atoms occupying alternate (111) planes.

In the $K_{0.7}CoO_2$ structure (*7*), the A atoms occupy trigonal prismatic sites with an oxygen packing sequence (*AB, BA* . . .). In $K_{0.5}CoO_2$ the sequence is (*AB, BC, CA* . . .).

In the delafossite ($CuFeO_2$) structure (*8*), the A atoms are in linearly coordinated sites between the BO_2 layers (Fig. 3). For A = Cu, Pd, Ag, the O–A–O bond is symmetrical, and for A = H the delafossite structure corresponds to the strongly hydrogen-bonded $HCrO_2$ structure (*9*).

B. Tunnel Structures

We have taken the $A_2Ti_6O_{13}$ structure (*A*

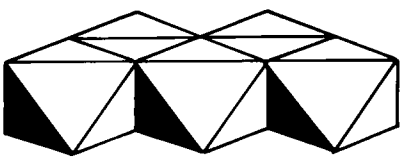

FIG. 1. Infinite BO_2 sheet.

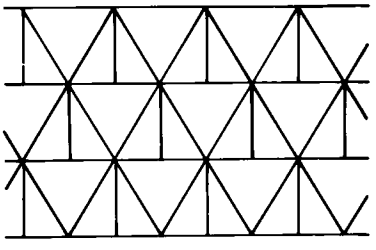

FIG. 2. α-$NaCrO_2$ structure; top and bottom sheets, CrO_2^-; Na^+ ions in octahedral interlayer sites.

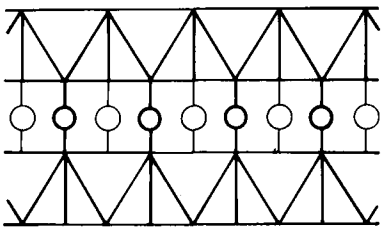

FIG. 3. $CuFeO_2$ (delafossite) structure; top and bottom sheets, FeO_2^-; unfilled circles, Cu^+ ions.

= Na, K, Rb, Cs) (*10*) as representative of this class. The structure is illustrated in Fig. 4; it contains one-dimensional tunnels enclosed by triple V_2O_5 chains sharing common corners (*11*).

C. Close Packed Anion Framework Structures

The β-$NaAlO_2$ and spinel structures were chosen as representative of framework phases containing a close packed anion array. In β-$NaAlO_2$ (*12*) the Na^+ and Al^{3+} ions occupy alternate tetrahedral sites of the hexagonal close packed wurtzite structure (Fig. 5). In the $A[B_2]O_4$ spinel phase there is an ordered arrangement of the metal atoms among the octahedral and tetrahedral interstices of a cubic close packed oxygen lattice.

3. Experimental

A. α-$NaCrO_2$

This compound was prepared by heating Analar Na_2CO_3 and Cr_2O_3 in the stoichiometric properties at 750°C for 12 hr under argon. The X-ray powder pattern (Cu $K\alpha$) measured on a Philips PW 1051 diffractometer with focussing monochromator, agreed with the published data (*6*). No other phase was detected, and the refined hexagonal parameters a = 2.971(1) Å, c = 15.96(1) Å were determined.

To attempt Li^+ ion exchange, α-$NaCrO_2$ was treated with an excess of Analar molten $LiNO_3$ for 24 hr at 300°C. The product was separated by treatment with deionized water and centrifuging. The collected washings were analyzed by atomic absorption spectroscopy for the sodium liberated; the analysis showed that ≈90% of the Na^+ had been exchanged by Li^+. However, the presence of an excess of Li^+ ions in the solution is known to interfere with the Na^+ ion analysis. Nevertheless, the result is consistent with substantial exchange having taken place. The Debye–Scherrer photographs of the product gave the d values shown in Table II, and the refined lattice parameters a = 2.902(1) Å, c = 14.44(1) Å for the exchanged product are in excellent agreement

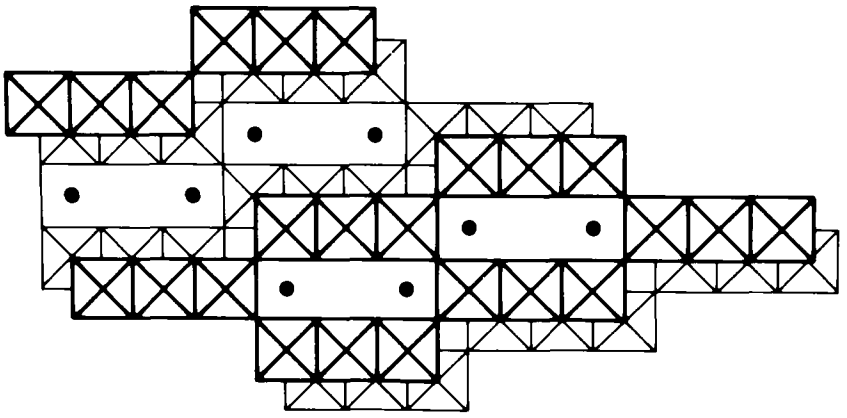

FIG. 4. $K_2Ti_6O_{13}$ structure; filled circles K^+ ions.

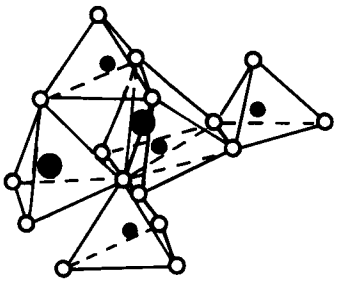

FIG. 5. Fragment of the β-$NaAlO_2$ structure; empty circles, O; small filled circles, Al; large filled circles, Na.

with the literature values (*6*) for α-$LiCrO_2$ (a = 2.905 Å, c = 14.44 Å). This experiment illustrates that rapid ion exchange is possible in the layered α-$NaCrO_2$ structure even in the absence of extensive cation vacancies.

Aqueous acid exchange was also investigated by treating α-$NaCrO_2$ with a 300-fold excess of 25% HNO_3 at room temperature for 12 hr. The extent of the exchange reaction.

$$NaCrO_2 + nH_2O + xH^+(aq) = H_xNa_{1-x}CrO_2 \cdot nH_2O + xNa^+(aq)$$

was followed by Na^+ atomic absorption analysis; 92% exchange was observed, and this did not appreciably alter with a second treatment. X-Ray diffraction of the H^+-exchanged product showed the presence of a poorly crystalline phase with peaks of ≈2° halfwidth. The new phase could be indexed on a hexagonal cell similar to that of α-$NaCrO_2$, but with altered lattice parameters (a = 2.96 Å, c = 14.2 Å). The c lattice parameter is significantly greater than that found in $HCrO_2$ (a = 2.98 Å, c = 13.40 Å), and TGA analysis to 800°C indicates a composition $HCrO_2 \cdot 0.92H_2O$. Heating the exchange product at 400°C yields $HCrO_2$. As the lattice expansion is not as large as expected for forming exclusively interlayer H_3O^+ ions, it is likely that a significant proportion of the water occupies interparticle regions. This is consistent with the X-ray evidence of small crystallite sizes, which normally results in substantial water sorption (*4*).

TABLE II

X-RAY POWDER DATA FOR α-$LiCrO_2$ OBTAINED BY ION EXCHANGE OF α-$NaCrO_2$

$h\,k\,l$	d_{obs}	d_{calc}	I
0 0 3	4.828	4.814	s
1 0 1	2.475	2.476	s
1 0 2	2.368	2.374	m
1 0 4	2.064	2.063	s
1 0 5	1.894	1.896	m
1 0 7	1.593	1.595	m
1 0 8	1.466	1.466	m
1 1 0	1.451	1.451	s
1 1 3	1.389	1.389	m

B. Related ABO_2 Structures

There are several experiments and measurements in the literature that are related to the above findings. The reaction

$$LiCoO_2 = Li_{1-x}CoO_2 + xLi$$

has been carried out electrochemically (*13*), and appreciable Li^+ ion mobility has been observed ($D_{300\ K} \approx 5 \times 10^{-9}$ cm^2 sec^{-1}).

The related $K_{0.72}[Sc_{0.72}Hf_{0.28}]O_2$ phase with the $K_{0.7}CoO_2$ structure, has been shown to be a poor ionic conductor at room temperature with $\sigma_{300\ K} = 4 \times 10^{-8}$ ohm^{-1} cm^{-1} and an activation energy for conduction E_A = 57.8 kJ mole^{-1} (*14*). An estimate of $D_{300\ K} \approx 10^{-10}$ cm^2 sec^{-1} can be made (vide infra) which is compatible with ion exchange at room temperature over several days.

Table III shows the reactions used by Shannon and co-workers (*8*) to prepare phases with the delafossite structure. Direct synthesis of the products was not possible, and the moderate temperatures used suggest that the reaction mechanisms involve ion exchange of the A ions and, where necessary, only an associated

TABLE III

ION-EXCHANGE REACTIONS OF LAYERED α-$NaCrO_2$ TYPE STRUCTURES (FROM (*8*))

Substrate	Structure	Reagent	Product	Structure
α-LiMO_2 (M = Co, Cr, Rh)	α-$NaCrO_2$	Pd + $PdCl_2$	PdMO_2	Delafossite
α-$LiFeO_2$	α-$NaCrO_2$	CuCl(l)	$CuFeO_2$	Delafossite
α-LiMO_2 (M = Co, Cr, Rh)	α-$NaCrO_2$	$AgNO_3$(l)	AgMO_2	Delafossite

change in the layer stacking sequence which can be accommodated by a small shear perpendicular to the c axis.

C. $A_2Ti_6O_{13}$

$K_2Ti_6O_{13}$ was prepared by a method similar to that of Wadsley (*10*). The X-ray powder pattern could be indexed on a monoclinic cell with lattice parameters (a = 15.61(4) Å, b = 3.796(2) Å, c = 9.12(2) Å, β = 99.0(1)°), close to the literature values.

Na^+ ion exchange was carried out at 850°C using an excess of molten Analar NaCl for a 12-hr period. The solid material was separated by treatment with H_2O and centrifuging. The observed and calculated d values of the product, which could be indexed with a monoclinic unit cell similar to that of $K_2Ti_6O_{13}$ are shown in Table IV. Refined monoclinic lattice parameters (a = 15.12(3) Å, b = 3.738(6) Å, c = 9.16(3) Å, β = 99.3(1)°) were in close agreement with those of directly synthesized $Na_2Ti_6O_{13}$ (a = 15.13 Å, b = 3.745 Å, c = 9.16 Å, β = 99.3° (*10*)) indicating complete exchange.

Li^+ ion exchange was first attempted by treating $Na_2Ti_6O_{13}$ with molten Li_2SO_4 at 900°C for 12 hr. The diffractometer trace showed the presence of TiO_2 and the cubic spinel $Li_4Ti_5O_{12}$, although the decomposition was probably preceded by ion exchange.

$$4Li^+ + 2Na_2Ti_6O_{13} = 4Na^+ + \underset{\text{metastable}}{2Li_2Ti_6O_{13}}$$

$$= 4Na^+ + Li_4Ti_5O_{12} + 7TiO_2$$

Li^+ ion exchange of $Na_2Ti_6O_{13}$ at the lower temperature of 280°C (using molten lithium nitrate) yielded a product whose X-ray pattern could be indexed on a monoclinic cell similar to that of $K_2Ti_6O_{13}$, though with changed lattice parameters. The observed and calculated d values are shown in Table V. The corresponding refined lattice parameters are a = 15.45(2) Å, b = 3.757(2) Å, c = 9.11(2) Å, β = 99.8°. The cell volume of the Li analog is anomalous in that it is slightly larger than that of $Na_2Ti_6O_{13}$. Since Na, K, and Rb are eight-coordinate in these phases, and eightfold coordination of Li^+ is unknown, the anomalous lattice parameters may be due to a coordination change for Li^+, possibly to a four-coordinate site. Also, the removal of Na^+ ions may not be complete. The possi-

TABLE IV

X-RAY POWDER DATA FOR $Na_2Ti_6O_{13}$ OBTAINED BY ION EXCHANGE OF $K_2Ti_6O_{13}$

h k l	d_{obs}	d_{calc}	I
2 0 0	7.468	7.463	s
$\bar{2}$ 0 1	6.292	6.275	m
1 1 0	3.629	3.617	m
$\bar{3}$ 1 0	2.981	2.989	m
$\bar{3}$ 1 1	2.931	2.923	m
$\bar{4}$ 0 2	2.671	2.674	m
$\bar{4}$ 0 3	2.546	2.555	vw
6 0 0	2.496	2.488	vw
$\bar{5}$ 1 2	2.185	2.190	w
$\bar{4}$ 0 4	2.085	2.089	m
$\bar{6}$ 0 2	2.043	2.045	m
$\bar{3}$ 1 4	1.899	1.894	w
0 2 0	1.868	1.869	m
2 2 1	1.774	1.772	vw
$\bar{5}$ 1 4	1.732	1.733	m

TABLE V

X-RAY POWDER DATA FOR THE PRODUCT OF Li^+ ION EXCHANGE OF $Na_2Ti_6O_{13}$

h k l	d_{obs}	d_{calc}	*I*
2 0 0	7.596	7.612	vs
$\bar{2}$ 0 1	6.394	6.366	m
$\bar{2}$ 0 2	4.191	4.192	w
4 0 0	3.786	3.805	w
1 1 0	3.648	3.648	s
$\bar{1}$ 1 1	3.480	3.428	w
1 1 1	3.339	3.332	vw
3 1 0	3.018	3.019	m
$\bar{3}$ 1 1	2.950	2.954	ms
3 1 1	2.780	2.778	w
4 0 2	2.683	2.686	m
$\bar{6}$ 0 1	2.557	2.558	m
$\bar{6}$ 0 2	2.386	2.390	w
$\bar{1}$ 1 3	2.359	2.362	w
1 1 3	2.276	2.268	w
$\bar{4}$ 0 4	2.096	2.096	m
6 0 2	2.065	2.064	m
0 2 0	1.879	1.878	m
2 2 0	1.821	1.824	w
$\bar{4}$ 0 5	1.743	1.742	w
7 1 2	1.650	1.651	m

bility of hydration of $Li_2Ti_6O_{13}$ was eliminated by a TGA study.

A 91% dense pellet of $Na_2Ti_6O_{13}$ was prepared by sintering a pressed pellet at 1200°C. The pellet was polished with 6 μm diamond paste, and gold blocking electrodes were applied. The AC impedance plots showed no evidence of ionic conductivity and no low frequency semicircular region. It was possible to set an upper limit of $\approx 10^{-8}$ ohm^{-1} cm^{-1} for the room temperature conductivity of this compound.

D. Spinel Phases

Joubert and Durif (*15, 16*) have reported the following ion-exchange reaction in an oxide spinel

$$(Li_{1.5}Zn_{1.5})_{tet}[Ge_{4.5}Li_{1.5}]_{oct}O_{12} = (Zn_3)_{tet}[Ge_{4.5}\square_{1.5}]O_{12}$$

The reaction conditions used were molten $ZnSO_4$ at 500°C for 3 weeks. The exchange was facilitated by the similar ionic radii of Li^+ (0.59 Å) and Zn^{2+} (0.60 Å) (*17*) in tetrahedral sites. It was of interest to attempt to reproduce this ion exchange with another spinel system, and we investigated the spinel $Li_4Ti_5O_{12}$, corresponding to $(Li_3)_{tet}[LiTi_5]_{oct}O_{12}$. A sample of $Li_4Ti_5O_{12}$ was supplied by M. R. Harrison of this laboratory. Its X-ray diffraction pattern could be indexed on the basis of a face-centered cubic unit cell with a = 8.357 Å. Ion exchange was carried out by treatment with molten $ZnCl_2$ at 500°C for 4 days. The product was separated by washing with dilute HCl and centrifuging. The washings were collected quantitatively for atomic absorption analysis of the Li^+ removed by ion exchange, the Li^+ standard solutions being prepared with an equivalent $ZnCl_2$ background present. This analysis showed that 68% of the Li originally present in $Li_4Ti_5O_{12}$ had been removed. The X-ray Debye–Scherrer photograph of the product showed the absence of any reflections due to $Li_4Ti_5O_{12}$; all but three reflections could be indexed on a primitive cubic cell with a = 8.405(5) Å. The corresponding d values are shown in Table VI together with the three unidentified reflections.

TABLE VI

X-RAY DATA FOR THE PRODUCT OF EXCHANGE OF $Li_4Ti_5O_{12}$ WITH MOLTEN $ZnCl_2$

h k l	d_{obs}	d_{calc}	*I*
1 1 0	5.965	5.915	m
2 0 0	4.157	4.188	w
2 1 0	3.740	3.749	m
2 1 1	3.414	3.422	mw
0 2 2	2.962	2.965	s
3 1 1	2.530	2.529	s
4 0 0	2.102	2.098	vw
4 2 2	1.714	1.714	m
3 3 3	1.615	1.616	ms
4 4 0	1.484	1.484	ms
Unindexed	3.531		m
Lines	3.246		mw
	1.685		w

Although the product was not single phase, there is clear evidence for an ion-exchange reaction having taken place. Primitive spinels, associated with cation ordering, have been observed by other workers. An example is $Li_2Zn[Ti_4Zn_2]O_{12}$, which has a similar lattice parameter (8.397 Å) to that observed here (*18*). It would seem most likely that exchange proceeds initially as

$$Li_3[LiTi_5]O_{12} \overset{Zn^{2+}}{=} Li_2Zn[\square Ti_5]O_{12}$$

where 50% of the lithium is released. The proportion of octahedral site vacancies is similar to that in $Zn_3[\square_{1.5}Ge_{4.5}]O_{12}$ (*17, 21*) and to γ-Fe_2O_3 which is approximately formulated as $Fe_3[\square Fe_5]O_{12}$ (*19*). Further exchange necessitates the creation of tetrahedral vacancies, which has not been observed in spinel systems. This may slowly occur, resulting in an extra release of lithium ions, but with the creation of an exchange-induced secondary phase.

The transport properties of spinels are compatible with these findings. Electrochemical insertion of Li into $Li_3[Ti_{\frac{1}{2}}Li_{\frac{1}{2}}\square_{\frac{1}{2}}]O_{12}$ has been shown (*20*) to produce a solid solution spinel phase for which the chemical diffusion coefficient $D \approx 10^{-7}$–10^{-8} cm^2 sec^{-1}. After the limit to the spinel structure is reached, $Li_3[Ti_{\frac{1}{2}}Li_{\frac{1}{2}}]O_{12}$, a defect rocksalt structure is ultimately formed, producing a limiting composition $Li_4Ti_3O_7$. In a study of $Fe_3[Fe_{4.5}Li_{1.5}]O_{12}$, Dudley and Steele (*21*) found evidence for Li^+ ion mobility. The ionic component of the conductivity was $\approx 6 \times 10^{-6}$ ohm^{-1} cm^{-1} at 295°C.

E. Close Packed Anion Framework Structures

It has not been generally appreciated that reactions in the literature may be interpreted as exchange reactions. Geissner and co-workers (*22, 23*) reported several such reactions, summarized in Table VII, in which various aluminates were treated with

TABLE VII

ION-EXCHANGE REACTIONS PRODUCING ORDERED-WURTZITE PHASES (FROM (*22, 23*))

Substrate	Structure	Reagent	Product	Structure
$KAlO_2$	Cristobalite	$AgNO_3$(l)	β-$AgAlO_2$	Wurtzite
$SrAl_2O_4$	Cristobalite	$AgNO_3$(l)	β-$AgAlO_2$	Wurtzite
$CaAl_2O_4$	Cristobalite	$AgNO_3$(l)	β-$AgAlO_2$	Wurtzite
γ-$LiAlO_2$	BeO	$AgNO_3$(l)	β-$AgAlO_2$	Wurtzite
β-$NaAlO_2$	Wurtzite	$AgNO_3$(l)	β-$AgAlO_2$	Wurtzite
β-$NaAlO_2$	Wurtzite	CuCl(l)	β-$CuAlO_2$	Wurtzite
β-$NaAlO_2$	Wurtzite	$TlNO_3$(l)	β-$TlAlO_2$	Wurtzite

melts containing Ag^+, Tl^+, or Cu^+ ions. The moderate reaction temperatures, below those normally necessary for reconstructive rearrangements, suggest an ion-exchange mechanism. In the reactions with ordered-wurtzite substrates and products, ion exchange involves the replacement of Na^+ or Li^+ ions with Cu^+, Tl^+, or Ag^+ ions on one set of sites in the structure. An interesting reaction is

$$Ag^+ + KAlO_2 = \beta\text{-}AgAlO_2 + K^+$$

where the stuffed cristobalite starting material is transformed to an ordered wurtzite phase. This is probably an exchange-induced reaction, the linear Al–O–Al bonds in stuffed cristobalite bending in a cooperative manner to trap the smaller Ag^+ ions in tetrahedral coordination.

4. Discussion

The kinetic and thermodynamic aspects of the exchange process are clarified by the schematic energy profile shown in Fig. 6. In step 1, partial exchange of component A with component A' is assumed to be thermodynamically favorable and to proceed by a relatively low activation energy. The temperature required to achieve a satisfactory rate of exchange is determined by the value of the relevant interdiffusion coefficient of the exchanging ions. At higher temperatures, either sintering or framework reconstruction occurs. Reconstruction will lead

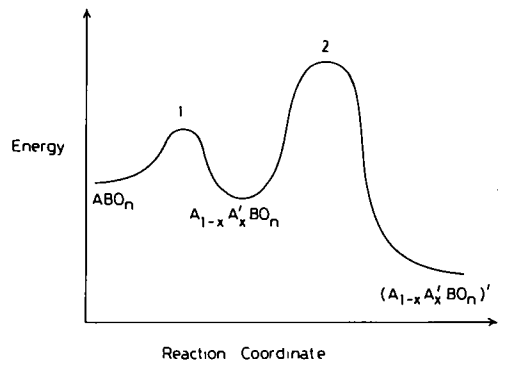

FIG. 6. Schematic energy profile of a low temperature ion-exchange reaction followed by a high temperature framework reconstruction.

to a new single or multiphase product and is represented by step 2 in Fig. 6.

The diffusion coefficient for single-ion diffusion has the form

$$D \approx n_v N^{-1} \gamma \nu_0 l^2 \exp(-\Delta G_m/kT)$$

where ΔG_m is the free energy change for ionic migration to an energetically equivalent (normally crystallographically equivalent) site; n_v is the number of vacancies per unit volume on these sites of total concentration N; γ is a geometrical term that may include any correlation factor; ν_0 is a mean optical-mode vibration frequency associated with the mobile ions; and l is the jump distance.

For a grossly nonstoichiometric phase n_v is a constant (extrinsic region) and

$$D = D_0 \exp(-\Delta H_m/kT)$$

where $D_0 = n_v N^{-1} \gamma \nu_0 l^2 \exp(\Delta S_m/k)$.

For a "stoichiometric" phase

$$n_v \approx N \exp(-\lambda \Delta G_f/kT)$$

where ΔG_f is the free energy change for vacancy formation and $\frac{1}{2} \leq \lambda \leq 1$.

Therefore, $D = D_0 \exp\{-(\Delta H_m + \lambda \Delta H_f)/kT\}$ where $D_0 = \gamma \nu_0 l^2 \exp\{(\Delta S_m + \lambda \Delta S_f)/k\}$.

The conductivity σ is related to D (strictly when the diffusion coefficient corresponds to charge transport) by the relation

$$\sigma = nq^2 D/kT$$

where n is the number of charge carriers per unit volume (approximately equal to N for a "stoichiometric" material and equal to $N - n_v$ for a nonstoichiometric compound), and q is the mobile ion charge.

Therefore, for a grossly nonstoichiometric material (extrinsic region) $\sigma = (A/T) \exp(-\Delta H_m/kT)$, where $A = k^{-1}\{n_v(1 - n_v/N)q^2 \gamma \nu_0 l^2 \exp(\Delta S_m/k)\}$. For a "stoichiometric" phase $\sigma = (A/T) \exp\{-(\Delta H_m + \lambda \Delta H_f)/kT\}$, where $A = k^{-1}[Nq^2 \gamma \nu_0 l^2 \exp\{(\Delta S_m + \lambda \Delta S_f)/k\}]$.

For a monovalent-ion conductor substitution of a typical value for n in the expression above indicates that $\sigma \approx 10^3 D$ for temperatures in the range 300–600 K. Therefore, from our earlier considerations, ion exchange is expected even for compounds with very low ionic conductivities ($\approx 10^{-9}$ ohm^{-1} cm^{-1}).

In the case of interdiffusion, where two different ions exchange places, the activation enthalpy for ion exchange may be as low as the larger ΔH_m for the two processes if extrinsic conduction is possible; it may be smaller than $\Delta H_m + \lambda \Delta H_f$ for a "stoichiometric" material supporting only intrinsic conduction if a ring diffusion process occurs. The latter is a feasible alternative for an ion-exchange process and would require a markedly lower activation enthalpy, for stoichiometric materials, than creation of vacancies; it is a mechanism whereby ion exchange can occur at an even faster rate than described by our previous equations.

The factors that influence ΔH_m include electrostatic, elastic, and geometric terms. The geometric term is defined by the "bottlenecks" through which an ion must pass to get from one site to another. If the distance of closest cation–anion approach is less than the sum of the ionic radii, then energy is required to open the bottleneck

wide enough for the mobile ion to pass through. The greater the required displacements of framework ions, the larger is ΔH_m. This simple consideration provides a useful criterion for identifying where ΔH_m must be too large for room-temperature exchange. In close packed structures, for example, the distance of closest cation–anion approach is ≤ 1.9 Å, defined by a common triangular face between intersticies of a close packed array. Whereas expansion of the separation between layers is possible in layered compounds such as $NaCrO_2$, the spinels and the $K_2Ti_6O_{13}$ structure are three-dimensional frameworks where the geometric constraints are not easily relieved. It is therefore not surprising that the activation energy for Li^+ ion mobility in the oxide spinels is too large for fast ion exchange at room temperature. However, at 500°C the Li^+ ion mobility in a close packed oxygen array appears to be significant; it is certainly large enough for practical ion exchange. Even more interesting is the Zn^{2+} ion mobility. In the systems chosen, the Zn^{2+} ion diffusion is facilitated by the exchange-induced cation vacancies; nevertheless, the rate of ion exchange of Zn^{2+} for Li^+ suggests a wider applicability of ion-exchange preparations than might have been anticipated. Also, with a relatively large activation energy, the rate of reaction increases markedly with increasing temperature. Thus, although large activation enthalpies produce extremely low room temperature values of D, the rapid increase in D with temperature may make practical ion-exchange reactions at temperatures near 500°C (see Table I).

Similar temperature dependent expressions for the diffusion coefficient may be derived for the case of solvated ion-exchange reactions in more liquid-like channels of expandable materials (*24*). In a hydrodynamic model, the exponential variation arises from the temperature dependence of the electrolyte viscosity; in a hole model, it arises from an activated hopping to a solvated cavity. Low enthalpies for ionic motion, and hence relatively large diffusion coefficients, are expected for this class of compound.

The experimental work in this paper has been concerned with ternary oxide phases containing small, highly charged cations (B) which, together with the anions, define the BO_n framework in which larger, less charged ions (A) are in interstitial postions. Substantial motion of the A ions is expected before that of the B ions particularly if the rigidity of the BO_n framework produces a high melting compound. The sintering/reconstruction temperature is then much higher than the temperatures used for molten salt reactions. Ion exchange in such materials may be anticipated even if they are nominally stoichiometric and have small bottlenecks to ion migration. The possibility of ion exchange is more suspect when the A and B atoms are comparable, in terms of size and charge and the material is relatively low melting.

In conclusion, fast ion conductors and practical ion-exchange resins, may undergo rapid ion-exchange reactions even at room temperature where aqueous, or nonaqueous exchange media can be used. Poorer ionic conductors may undergo ion-exchange reactions at higher temperatures where molten salts are applicable. Only extremely poor ionic conductors require reaction temperatures for ion exchange that compete with sintering temperatures for the host matrix. At these temperatures the energy barrier to reconstruction of an exchanged material may be overcome, assuming that such a phase change is thermodynamically viable (step 2 of Fig. 6). Our experimental findings corroborate theoretical considerations and confirm that the constraints applicable to fast ion conductors are much less stringent for ion exchange. Also, practical ion exchange has been demonstrated in stoichiometric mate-

rials having relatively small bottlenecks. Ion-exchange reactions thus appear to offer important, largely unexplored routes, for preparative solid state chemistry; they also appear to play an unrecognized mechanistic role in some solid state reactions. While the exchange reaction is conceptually simple, factors such as the extent of exchange, $F(\infty)$, and the possibility of concurrent water sorption are not easy to predict in advance. Therefore, the products of ion exchange require a thorough analysis and characterization.

References

1. Y. F. Yu Yao and J. T. Kummer, *J. Inorg. Nucl. Chem.* **29,** 2453 (1967).
2. G. E. Boyd, A. W. Adamson, and L. S. Myers, *J. Amer. Chem. Soc.* **69,** 2836 (1947).
3. D. Reichenberg, *J. Amer. Chem. Soc.* **75,** 589 (1953).
4. W. A. England, M. G. Cross, A. Hamnett, P. J. Wiseman, and J. B. Goodenough, *Solid State Ionics* **1,** 231 (1980).
5. D. Mapother, H. N. Crooks, and R. Maurer, *J. Chem. Phys.* **18,** 1231 (1950).
6. W. Rüdorff and H. Becker, *Z. Naturforsch. B* **9,** 614 (1954).
7. C. Delmas, C. Fouassier, and P. Hagenmuller, *J. Solid State Chem.* **13,** 165 (1975).
8. R. D. Shannon, D. B. Rogers, and C. T. Prewitt, *Inorg. Chem.* **10,** 713, 719 (1971).
9. W. C. Hamilton and J. A. Ibers, *Acta Crystallogr.* **16,** 1209 (1963).
10. S. Andersson and A. D. Wadsley, *Acta Crystallogr.* **15,** 194 (1962).
11. P. G. Dickens and P. J. Wiseman, M. T. P., *Int. Rev. Sci. Ser. 2 Inorg. Chem.* **10,** 211 (1975).
12. J. Théry, D. Briançon and R. Collongues, *C.R.* **252,** 1475 (1961).
13. K. Mizushima, P. C. Jones, P. J. Wiseman, and J. B. Goodenough, *Mater. Res. Bull.* **15,** 783 (1980).
14. C. Delmas, C. Fouassier, J. M. Réau, and P. Hagenmuller, *Mater. Res. Bull.* **11,** 1081 (1976).
15. J. C. Joubert and A. Durif, *Bull. Soc. Fr. Miner. Cristallogr.* **87,** 517 (1964).
16. J. C. Joubert, *Bull. Soc. Fr. Miner. Cristallogr.* **90,** 598 (1967).
17. R. D. Shannon and C. T. Prewitt, *Acta Cristallogr. B* **25,** 925 (1969).
18. M. C. Chaussy, H. Vincent, and J. C. Joubert, *Bull. Soc. Chem. Fr.* 198 (1966).
19. G. W. van Oosterhout and C. J. M. Rooijmans, *Nature (London)* **181,** 44 (1958).
20. B. E. Liebert and R. A. Huggins, "Second International Meeting on Solid Electrolytes," St. Andrews, United Kingdom (1978).
21. G. J. Dudley and B. C. H. Steele, *J. Electrochem. Soc.* **125,** 1994 (1978).
22. E. Thilo and W. Geissner, *Z. Anorg. Chem.* **345,** 151 (1966).
23. W. Geissner, *Z. Anorg. Chem.* **352,** 145 (1967).
24. J. O'M. Bockris and A. K. N. Reddy, "Modern Electrochemistry," Plenum, New York (1970).